Connection Science

ISSN: (Print) (Online) Journal homepage: https://www.tandfonline.com/loi/ccos20

Evolutionary computation for bottom-up hypothesis generation on emotion and communication

Casper Hesp , Bram T. Heerebout & R. Hans Phaf

To cite this article: Casper Hesp , Bram T. Heerebout & R. Hans Phaf (2020): Evolutionary computation for bottom-up hypothesis generation on emotion and communication, Connection Science, DOI: 10.1080/09540091.2020.1814203

To link to this article: https://doi.org/10.1080/09540091.2020.1814203

Published online: 09 Sep 2020.

CONNECTION SCIENCE
https://doi.org/10.1080/09540091.2020.1814203

Evolutionary computation for bottom-up hypothesis generation on emotion and communication

Casper Hesp, Bram T. Heerebout and R. Hans Phaf

Department of Psychology, University of Amsterdam, Amsterdam, NL, The Netherlands

ABSTRACT

Through evolutionary computation, affective models may emerge autonomously in unanticipated ways. We explored whether core affect would be leveraged through communication with conspecifics (e.g. signalling danger or foraging opportunities). Genetic algorithms served to evolve recurrent neural networks controlling virtual agents in an environment with fitness-increasing food and fitness-reducing predators. Previously, neural oscillations emerged serendipitously, with higher frequencies for positive than negative stimuli, which we replicated here in the fittest agent. The setup was extended so that oscillations could be exapted for the communication between two agents. An adaptive communicative function evolved, as shown by fitness benefits relative to (1) a non-communicative reference simulation and (2) lesioning of the connections used for communication. An exaptation of neural oscillations for communication was not observed but a simpler type of communication developed than was initially expected. The agents approached each other in a periodic fashion and slightly modified these movements to approach food or avoid predators. The coupled agents, though controlled by separate networks, appeared to self-assemble into a single vibrating organism. The simulations (a) strengthen an account of core affect as an oscillatory modulation of neural-network competition, and (b) encourage further work on the exaptation of core affect for communicative purposes.

ARTICLE HISTORY
Received 3 February 2020
Accepted 12 August 2020

KEYWORDS
Emotion; affective communication; evolutionary computation; genetic algorithms; neural oscillations

> Evolution behaves like a tinkerer who, during eons upon eons, would slowly modify his work (. . .)
>
> Jacob (1977, p. 1164)

The multi-faceted nature of emotions is illustrated by the very large number of different emotion theories (at least 150; Strongman, 1996), of which a synthesis does not seem to be forthcoming. Similar to most computational models, these theories mainly have been constructed from a top-down engineering stance. Biological emotions, however, have developed through bottom-up evolutionary tinkering (cf, Jacob, 1977). Evolution does not follow a pre-conceived plan but tends to select for whatever solutions happen to meet current

CONTACT R. Hans Phaf r.h.phaf@gmail.com Brain and Cognition Group, Department of Psychology, University of Amsterdam, PO Box 15915, 1001 NK, Amsterdam, The Netherlands

environmental demands best within the population at hand. It does not produce novelties from scratch but builds on previous phenotypes. Serendipitously, these can afford new functions through repurposing (i.e. exaptation; Gould, 1991), either gradually or through sudden leaps of reorganisation (e.g. Minelli et al., 2009). Few studies have engaged in evolutionary modelling of emotions, and these certainly have not been able yet to reach the level of full emotions.

This computational study first addresses the fundaments of any bottom-up approach to emotions, the development of core affect. Furthermore, to venture into the social aspects of emotions, we explored how affect can be employed adaptively in communication. Most models and theories consider affective quality, or positive and negative valence, the core of human emotions, but only very few present an explanation in terms of processes and mechanisms. Similar to the concept of time in physics, affect is predominantly thought of as an intuitively obvious concept that resists further analysis. In reinforcement learning models of emotions for instance, gains and losses (i.e. utility) are accepted as given basic elements (see Broekens et al., 2015). We believe that a deeper evolutionary analysis allows for a much broader construction of theories on emotional processes, extending beyond the behaviourist domain. Phaf and Rotteveel (2012) in their affective monitoring framework, broke down affect in terms of basic neural-network processes that can also be found in non-human animals, due to their shared evolutionary origins. In the current paper, affect is used to denote a fundamental neural process rather than to describe some form of human mental experience. Affective monitoring was based on the evolutionary understanding of positive and negative affect as coding respectively fitness-enhancing and fitness-reducing conditions (see Jacob, 1977; Johnston, 2003). Evolutionary reasoning also gave rise to the notion that the most important motivational tendencies are approach and avoidance, which roughly, but not always, correspond to positive and negative affect, respectively (cf, Phaf et al., 2014).

To investigate whether this type of evolutionary reasoning really sticks, an early study employed a Genetic Algorithm (Goldberg, 1989; Magnani & Bertolotti, 2017) to simulate the evolutionary development of artificial neural networks controlling virtual agents in a simple environment (den Dulk et al., 2003). This work was inspired by the well-known dual-route model for fear processing of LeDoux (1996), which assumes a "quick and dirty" direct route and a slower but more elaborate indirect route to the amygdala (for a critical evaluation of dual-route computational models, see Lowe et al., 2009). Interestingly, LeDoux motivated this model with the evolutionary reasoning that the fitness costs of false alarms to potential threats are smaller than of misses. Under these evolutionary pressures, in the simulations of den Dulk and collaborators organised approach and avoidance actions and a dual-route architecture emerged autonomously from initially disordered behaviour and zero connection weights. A short and crude path yielded fast and generalised avoidance responses whereas a slower pathway, which ran via an extra layer of hidden neurons, made a finer distinction. The longer pathway enabled either switching to an approach response (i.e. in the presence of food stimuli), or strengthening the fast avoidance response (i.e. if a predator was detected).

Newer work from our group, in which the longer network path was extended with a second hidden layer recurrently connected to the other hidden layer, led to the serendipitous discovery that neural oscillations markedly improved the agents' ability to avoid predators and collect food (Heerebout & Phaf, 2010a, 2010b). The networks manifested higher

frequency oscillations in the presence of fitness-increasing stimuli (i.e. food sources) than with fitness-reducing stimuli (i.e. predators). From a theoretical analysis, rather than from an evolutionary emergence, Burattini and Rossi (2010) inferred a somewhat similar role of oscillations in the emotional modulation of action tendencies. Interestingly, these authors also tested their ideas in a predator/prey environment where agents (i.e. robots) had to select from conflicting actions when facing the two types of stimuli.

The surprising finding of affective frequency coding even received empirical support, not only showing that high-frequency neural oscillations (i.e. in the Gamma band) accompany positive affect (Kounios & Beeman, 2009; Marco-Pallarés et al., 2015) but also that these oscillations can induce positive affect (in mice: Tsai et al., 2009; in humans: Heerebout et al., 2013). Further analyses revealed that oscillations modulated neural competition, which has been invoked as the central mechanism in attention (Cerf et al., 2010; Duncan, 1996). High frequencies facilitated switching between competition winners, whereas low frequencies led to more rigidity. When being hunted, it is beneficial for survival not to be distracted by food (i.e. "it is better to miss dinner than to be dinner"). Conversely, while foraging it is beneficial to be able to respond quickly to an approaching predator. Oscillation frequency, thus, emerged in these simulations as a neural code for positive and negative affect (Jacob, 1977; Johnston, 2003; cf, Phaf & Rotteveel, 2012).

We conjecture here that basic communicative behaviours employ (i.e. exapt; Gould, 1991) these frequency codes for positive and negative affect. The frequencies of ultra-sonic vocalisations (USVs) produced by rats, for instance, show a remarkable correspondence, with USVs of 50 kHz during appetitive situations and of 22 kHz during aversive situations (Wöhr et al., 2015). These emotional expressions are more pronounced when an "audience" of conspecifics is present (as in humans, Fridlund, 1994). The vocalisations persist after lesioning the cortex and hippocampus, suggesting that they rely largely on evolutionarily older subcortical regions, suggesting that they are based on an inherited predisposition. The prevalence of affective signalling in many species indicates that this ability contributes to survival under large environmental variations. Speculatively, the frequency-dependent characteristics of USVs could have originated from a pre-existing distinction in underlying neural mechanisms. As was already argued by Darwin (1872) in his principle of associated serviceable habits, these expressions could have developed from a simpler function through a process of ritualisation and exaptation to a social function (Gould, 1991; Shariff & Tracy, 2011).

This computational study aims to explore the evolutionary tinkering of communication starting from an evolutionary generation of core affect. Previous evolutionary simulation studies into communication either did not share this starting point (e.g. de Greeff & Nolfi, 2010; Di Paolo, 2000), or investigated affective signalling with pre-programmed communicative functions that could not develop autonomously (e.g. Reggia et al., 2001). We adapted the setup of Heerebout and Phaf (2010a, 2010b) to study the potential emergence of affective signalling when two agents navigate the environment simultaneously and are equipped with new actuators and receptors to potentially sense and signal each other. To meet the increased demands for computational resources by this extension, the simulations were performed on a computer with 8-core CPUs. This parallelisation also entailed some modifications to the genetic algorithm and the software, which called for a replication of previous simulation work to ensure that the same frequency coding of affect would emerge. In Simulation 1, we attempted to replicate the single-agent findings of Heerebout

and Phaf (2010a, 2010b) in a slightly modified setup and when using different hardware and software. In Simulation 2, we studied whether the extension of the setup of Simulation 1 with a second agent would enable the generation of a form of affective signalling involving oscillations. Replicating the generation of neural oscillations in the first part would thus allow us to study their exaptation for affective signalling in the second part.

Materials and methods

Simulation 1. Neural oscillations

The setup of the evolutionary simulations of Heerebout and Phaf (2010ab) was implemented in a computer with 8-core CPUs with a few changes to the genetic algorithm and rewritten in the flexible programming language Python (van Rossum & Drake, 2001).

Agent body and neural architecture

Figure 1a shows the agent's circular body and neural architecture. Both sides have nostrils registering scent intensity and a motor actuator. The network has four input nodes (two scent types per nostril) and two output nodes driving the motor actuators. Input and output layers are connected directly, and indirectly through a hidden layer of four nodes. The hidden layer has bidirectional (i.e. feed-forward and feed-back) connections with a four-node context layer. The agent's "DNA" determines the connection weights, which would not change during its lifetime. Furthermore, to halve the search space, the networks are bilaterally symmetric. As a result, a stimulus to the left produces an identical, but mirrored, response as a stimulus on the right. Agents initially have five energy units and could gain more by eating plants. Time and movement, however, cost energy. An agent would die whenever it ran out of energy or collided with a predator.

Environment setup

The two-dimensional environment (see Figure 1b) formed a square containing at random initial locations ten plants, and six predators with the same size and round shape as the agents. Plants spread two scents (scents A and B; see Appendix A) in proportion 1:2, whereas the predators did so with proportion 2:1. The overlapping scent patterns ensured that distinguishing between plants and predators was a non-trivial task. The agents emitted a third scent (scent C) that could only be sensed by the predators, which were programmed to chase the agents through a fixed network architecture. The neural network controlling the predators only had an input and an output layer with pre-set connection weights (see Appendix E), such that they chased agents (scent C) and avoided each other (scent D). The predators did not experience any delay in the transmission of activations to the output layer, so that their processing speed was higher than of the agents.

Genetic algorithm

The first generation consisted of 18 agents with all connection weights (the DNA) set to zero. Early in the evolutionary simulations, the agents, therefore, showed random, disorganised behaviour. In every generation, each agent was tested twelve times. The fitness was calculated by multiplying the energy at death by the survival time (averaged over

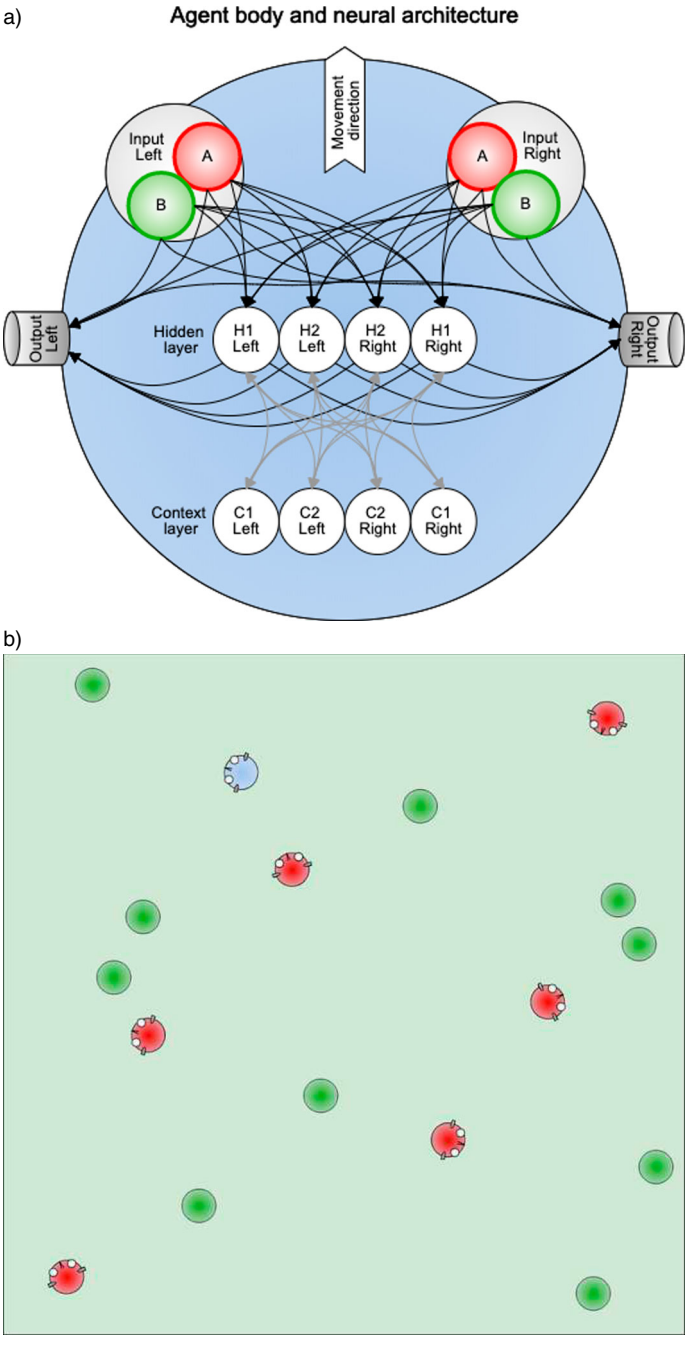

Figure 1. a) the agent's body and neural architecture. The nostrils are located on the top as the input nodes for scents A (red, emitted mostly by predators) and B (green, emitted mostly by plants). The motor actuators are output nodes located on the left and right sides. b) an example environment with one agent (blue), six predators (red) and ten plants (green).

twelve tests). Two parents were then selected to generate new agents several times until the population size had tripled.

The first selected parent was the fittest agent of a random one-third subset of the population (i.e. tournament selection). The second parent was chosen with a probability proportional to its fitness and inversely proportional to its difference from the first (i.e. Euclidic distance between the agents' weights). The main contributor to the DNA was randomly chosen from these two parents. The probability for crossover to occur was 0.5, in which case the least-contributing parent would determine only two (randomly chosen) connection coefficients. All weights were subjected to random mutations of average size 0.1 (see Appendix B, for the precise function), keeping the absolute value of the connection weights below 10.

About two-thirds of each triple-sized population (containing parents and offspring) was discarded as a function of fitness relative to the population fitness range and population size (see Appendix C), allowing the population size to change along with population fitness variations. At this point, the next triple-sized generation would be produced (10,000 generations were deemed sufficient by Heerebout & Phaf, 2010b). Simple parallelisation in the 8-core CPU sped up the code sixfold but required equal numbers of agents for all the sub-groups running in parallel. We adopted the Champion method by filling up remaining slots with copies of the fittest agent across all previous generations (i.e. the current champion).

Analysis of the final population

The agents from the final population were placed in a test environment with a single plant or predator that was placed directly in front of the agents (and slightly to the left, to prevent fully symmetric input). The activations of the individual nodes were then recorded over time (i.e. in terms of number of time steps) together with the agent's distance to the stimulus.

Simulation 2. Inter-agent signalling

The method of Simulation 2 was largely similar to Simulation 1, so in the following, we will only describe and motivate the differences.

Dual agent body and neural architecture

Oscillating neural networks were taken as the starting point of this simulation by setting the weight configurations of the initial population equal to the highest fitness agent that evolved in Simulation 1. To limit the search space moreover, the two agents were genetically identical in all generations. This simulation investigated the potential interaction of agent pairs within the environment. We aimed for the simplest form of communication possible by introducing a single new scent type E, which the agents could emit and sense. To strengthen the potential utility of communication, we extended the spatial range of the communication scent (see Appendix D) beyond the ranges of food and predator scents (cf, Reggia et al., 2001), so that communication could serve as a warning signal before a stimulus is detected. Agents were equipped with an output node serving as emitter and two additional input nodes (one for each nostril) sensing the intensity and direction of scent E. The new input nodes connected directly to the output nodes of the motor actuators and to

the hidden layer. The new, scent-emitting, output node received input only from the hidden layer (see Figure 2a). The new parts of the networks were initialised with connection weights set to zero.

Environment setup

To increase the need for communication, the environment was enlarged by 50%and contained fewer stimuli than in Simulation 1. To enable sharing spatial information, the environment was no longer homogeneous but structured into different zones (see Figure 2b). The foraging zone, containing four plants, was in the bottom left with a width and height of 20 times the agent's radius. The four predators were confined to a square area on the top right of 40 times the radius. The remaining two strips contained no food or predator stimulus but could be roamed by the agents.

Genetic algorithm

Simulation 1 indicated that the mutation size might have been too large for this weight configuration to remain stable. The average mutation size was consequently reduced by a factor 10. The need for cooperation between agents was enhanced by making the survival of each agent contingent on the survival of the other. Whenever one of them starved to death or was eaten by a predator, both would be removed from the environment. However, the agents had separate energy budgets and needed to gather food individually. The fitness value of each pair was obtained by multiplying energy at death of both agents with their lifetime, averaged over twelve tests.

Analysis of the final population

The first step in the analysis was to compare the fitness development across generations of populations with and without communicative abilities. The communicative network parts were also lesioned and the fitness distributions were compared before and after lesion. For pairs that revealed an adaptive communicative function, we analysed how they achieved higher fitness. A logical starting point was simply to visualise the behaviour of the agents within the simulations, along with their network activations, and look for patterns of mutual coordination.

Next, we set up a reduced environment as in the analysis of Simulation 1. To reveal whether any form of communication had emerged, an agent (labelled agent Y) of each pair was placed in a testing environment with either food or a predator (both stationary), in the presence or absence of a stationary conspecific (labelled agent X). The stimuli were initially placed close to X but on the border of the perceptual range of Y. Because the communication scent had a much larger range, this setup allowed any signals from X to be processed by Y before the weak input from the stimulus would reach it. Two different initial locations of either stimulus were chosen, either on the direct path from X to Y or perpendicular to that path (see bottom row of Figure 7).

Finally, internal network dynamics were studied by pruning (i.e. setting weights below a certain threshold to zero) and analysing the processing in the remaining network. This could reveal the presence of node competition (cf, Heerebout & Phaf, 2010a). Competition between nodes is usually indicated by lateral inhibitory connections, such that the nodes can suppress one another, and the most strongly activated node wins. The present neural networks do not possess horizontal connections however, but the same competitive result

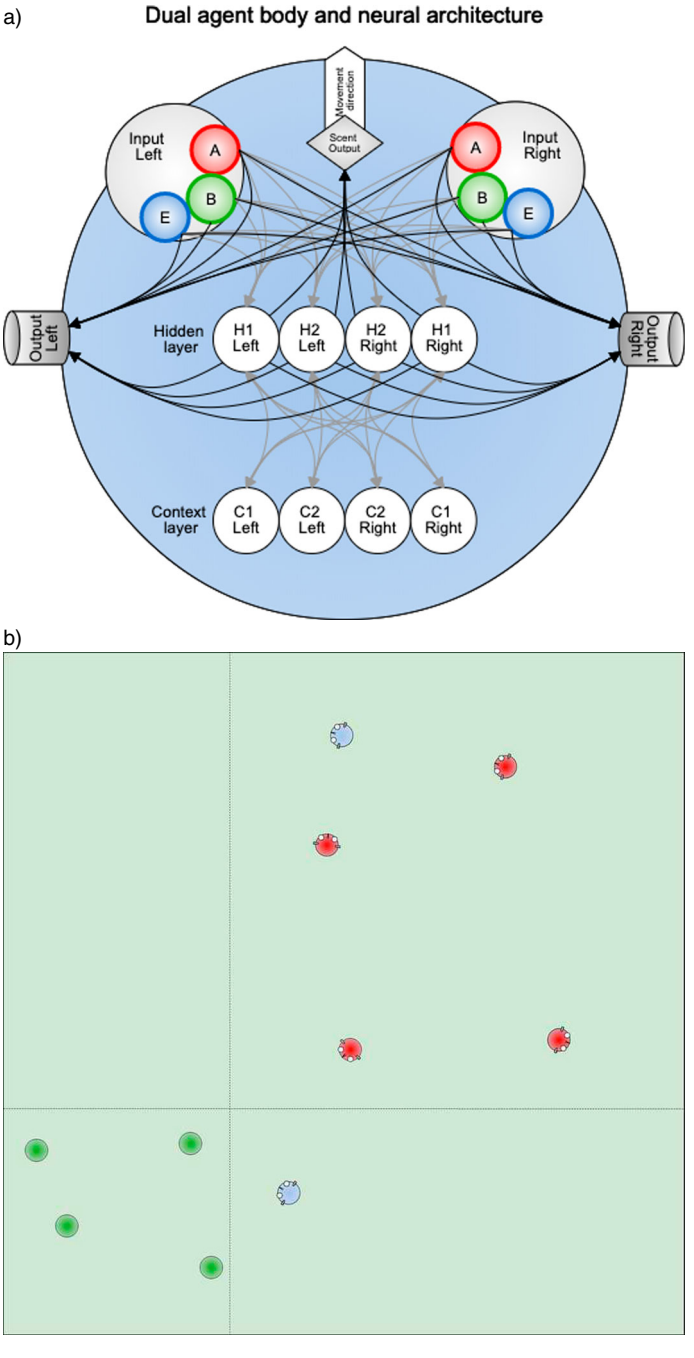

Figure 2. The agents' body and neural architecture (a), and an example initial environment (b) in Simulation 2. The scent-input nodes (nostrils) are located on the left and right front side (communication scent E in blue), the diamond-shaped scent-output node on the top. The environment contains two agents (blue), four plants (green), and four predators (red). The agents, but not the predators, could travel freely across all areas.

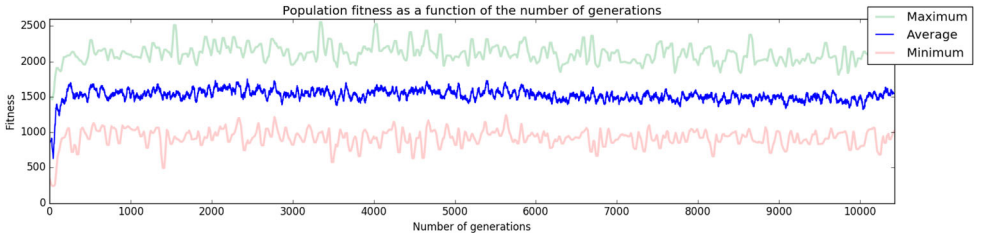

Figure 3. The population fitness (in units of energy x lifetime) in Simulation 1 as a function of generation (over 10,371 generations). The curve was smoothened using a window of 50 generations (resulting in the blue line). The smoothened maximum (green) and minimum (red) fitnesses are also depicted.

can be achieved indirectly through recurrent connections from the context layer. A hidden-layer node, for instance, could activate through an excitatory connection a context-layer node that inhibits one of the other hidden-layer nodes, this suppressing the activation of this node.

Results

Simulation 1. Neural oscillations

Simulation 1 replicated the findings of Heerebout and Phaf (2010b), only with respect to the fittest agent. After 10,371 generations, the population consisted of 22 agents, with an average fitness of 1,649 (energy x lifetime). As Figure 3 shows, the fitness reached a maximum early (at around 300 generations) and fluctuated for the remainder of the simulation. Heerebout and Phaf (2010a) reported a sudden jump in fitness, but also sometimes observed a more gradual emergence of oscillations. Forty-one per cent of the final population showed neural oscillations in response to the stimulus, and 27% only when moving away from the stimulus. Only the fittest agent (fitness 1,915) showed higher frequencies for positive (i.e. food) than negative (i.e. predator) stimuli (ratio 2:1). The high fitness indicates that this configuration with distinctive high and low-frequency oscillations is particularly adaptive under these environmental selection pressures.

Oscillation frequencies with plants and predators

Food or predator stimuli were placed at a fixed location slightly to the left of the fittest agent. The node-activation patterns of the moving agent are shown in Figure 4. In the first few time steps, the agent always started to move forward, which resulted in an initial distance reduction to the stimulus. Subsequently, approach or avoidance behaviours are performed to the food and predator stimuli, respectively. At about time step 14 the plant is eaten (left column, Figure 4). The agent of course, never collides with the predator and moves away from it. In response to the plant, the agent immediately showed high-frequency oscillations in its hidden and context layers. The differential oscillating spikes of the left and right output nodes to the motor actuators drive the agent to approach the plant. At time step 14 the agent eats the plant and continues to move forward due to the left and right oscillation peaks having equal amplitude. Oscillations in response to the predator

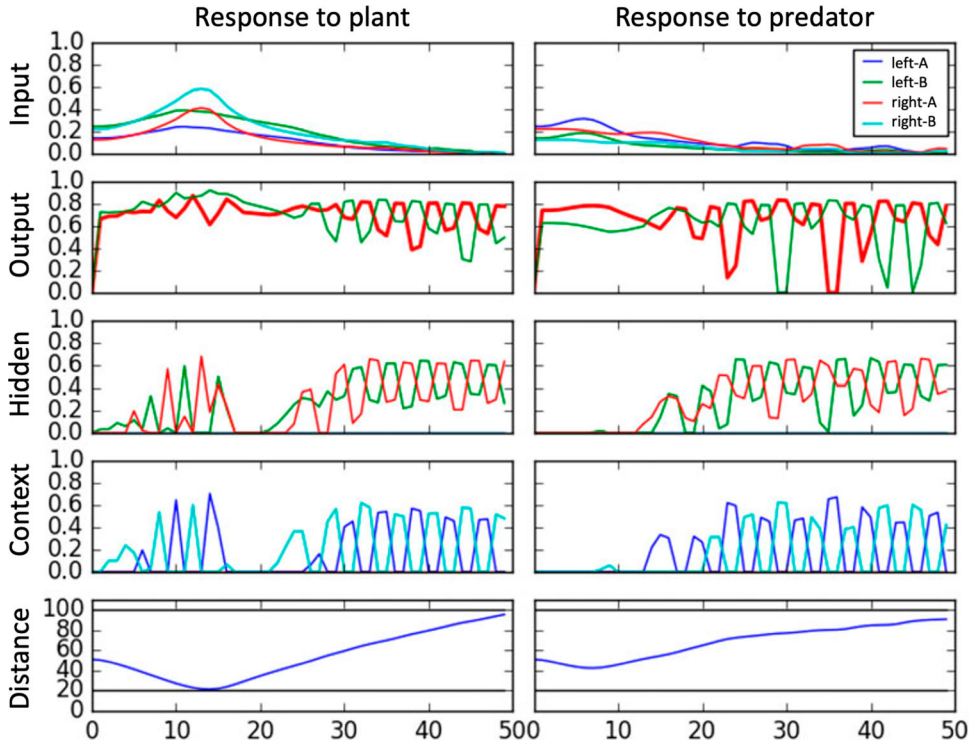

Figure 4. Recordings of node activations and agent-stimulus distance as a function of time (number of time steps on the horizontal axis) from the fittest agent due to a plant stimulus (left column) and a predator stimulus (right column). The top row shows the input activations for the left nostril (scent A in blue, scent B in green) and the right nostril (scent A in red, scent B in cyan). The second row shows the output activations for the left and right actuator (red and green) and the third and fourth rows show oscillating activations nodes in the hidden and context layer. The bottom row shows the distance between stimulus and agent. The black horizontal lines indicate where agent and stimulus touch (at distance 20) and where the maximum range of the scent is reached (at distance 100).

started later, with half the frequency. Here the amplitude difference between left and right peaks prompts avoidance.

In conclusion to Simulation 1, our findings demonstrated that it is possible to replicate the findings of Heerebout and Phaf (2010a, 2010b) in a different programming language and with changes to the genetic algorithm. This also strengthens the mechanical analysis of core affect in terms of oscillations and competitive neural processing (Phaf & Rotteveel, 2012; see also General Discussion). In the final population, neural oscillations were present abundantly. Supporting previous findings, the agent that was by far the fittest indeed exhibited higher frequencies with positive than with negative stimuli. This phenotype was observed only once in the final population. Most likely, the neural mechanism that produced differential frequencies might have been too vulnerable to mutations here. This point finds additional support in the extensive fluctuations of the population fitness across

Table 1. Group-averaged fitness values F and time percentages spent by the final population in the zones for food (T_{food}), predators (T_{pred}), and no stimulus (T_{none}). The same is shown for subgroups of oscillatory (A) and non-oscillatory pairs (B). The latter subgroup is subdivided into pairs with fitness values below (i.) and above (ii.) the population mean ($F_{pop} = 3{,}525$).

Agent group	N	F (E_f x T_{tot})	T_{food} (%)	T_{pred} (%)	T_{none} (%)
Entire population	36	3,525	26.7	7.1	66.2
A. Oscillatory	17	2,169	19.1	8.3	74.6
B. Non-oscillatory	19	4,740	33.5	6.1	58.7
i. $F < F_{pop}$	15	2,714	31.2	6.3	60.4
ii. $F > F_{pop}$	4	12,335	42.0	5.5	52.5

generations (see Figure 3). However, this can also partly be explained by (random) environmental variation, which was due to the agents and stimuli being located randomly across generations.

Because differential frequencies only emerged in a single agent, the chances that they could be exapted reliably into a communicative function would be rather slim when starting from scratch as in Simulation 1. In nature, genetic stability can be enhanced by mechanisms that limit the proliferation of spontaneous mutations (cf, Drake et al., 1998). If a specific gene is beneficial but very vulnerable to mutations, the advantage can be maintained through new mutations that reduce the overall mutation rate. Similarly, the mutation size could be coded into the agents' genes here, so that evolutionary selection can act on the mutation size. This would markedly increase the search space of the genetic algorithm however and would go beyond the scope of the current study. Therefore, to limit the search space in Simulation 2, we started with the most successful genetic configuration in the initial agents (i.e. the highest fitness agent from Simulation 1), while reducing the average overall mutation size.

Simulation 2. Inter-agent signalling

Comparison with control and lesion simulations

After 9,313 generations, the population consisted of 36 agent pairs, with an average fitness value of 3,525 (E_1 x E_2 x T_{life}), as compared to 2,344 for the reference simulation with non-communicative dual agents. The average fitnesses diverged within the first 500 generations (see Figure 5). Subsequently, the communicative pairs fluctuated around a value of 3,300, whereas the reference pairs remained relatively stable at about the 2400 level.

The fitness increase of the communicative agent population was due to specific pairs (see Figure 6 and Table 1) reaching much higher fitness values than the rest (i.e. up to 10 times higher). To establish whether the difference was caused by the communicative abilities, we lesioned the connections (i.e. set to zero) necessary for communication in each pair (for the fitness values before and after lesion, see Figure 6). The lesion only affected the fittest individuals, and the average fitness after lesion (2,300) was comparable to that of the non-communicative reference simulation (2,344).

Table 1 summarises the final population in terms of fitness values and total time percentages spent in the food, predator, and stimulus-free zones. It came out that oscillatory activity did not confer any fitness benefit in the simulation. The non-oscillatory pairs clearly

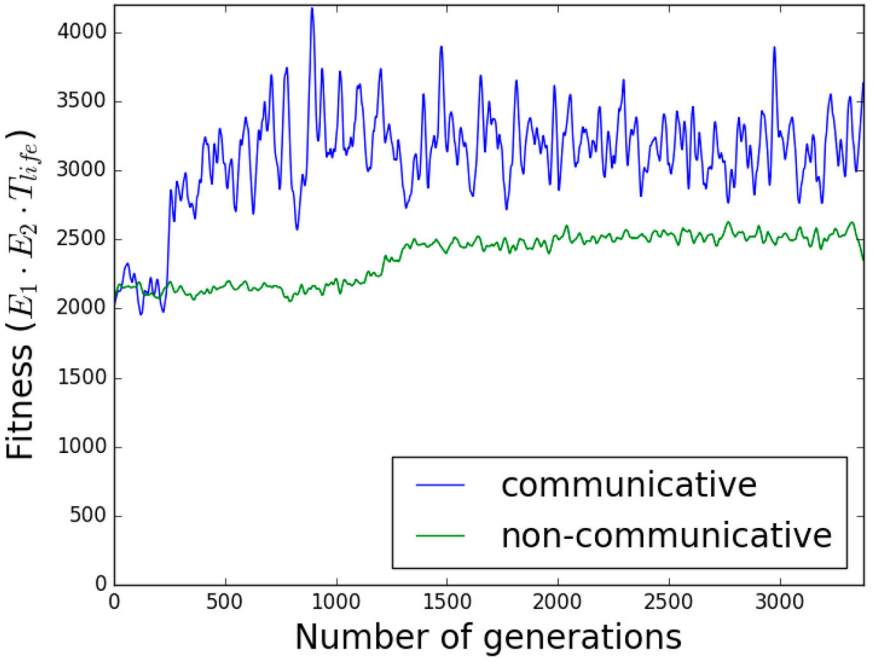

Figure 5. The average population fitness in Simulation 2 as a function of generation, for communicative (blue) and non-communicative agents (green). The curve was smoothened using non-parametric smoothing (cf, Cleveland, 1979).

reached higher fitness levels than the oscillatory agents. Instead, the high-fitness group appeared to spend much more time in the food zone and less time in the predator zone than the other groups.

Behaviour of the fittest pair

Within the full simulation, we observed general approach behaviour of the fittest agents. In the absence of any stimulus, these pairs moved periodically almost along a straight line. The agents approached each other, passed through each other (they could not collide), and quickly turned around to repeat these actions. In the presence of stimuli, the agents also joined, but they moved in a circular pattern with stimulus-specific deviations, which resulted in a net movement of the couple towards food sources and away from predators. It seemed almost as if the agents were vibrating along a virtual leash (see Figure 7), a connection that became looser in the presence of other stimuli. These flexible movement patterns functioned both to avoid rapidly approaching stimuli (i.e. predators) and to approach stationary stimuli (i.e. plants). Their joint spiralling movement served to circumvent approaching predators because the latter could not home in on a single agent. Conversely, the successful pairs managed to jointly spiral towards a stationary food source. The mutual coordination between agents, thus, depended on stimulus valence. According to Michael (2011), this kind of affect detection is one of the coordinating factors in shared emotion and joint action.

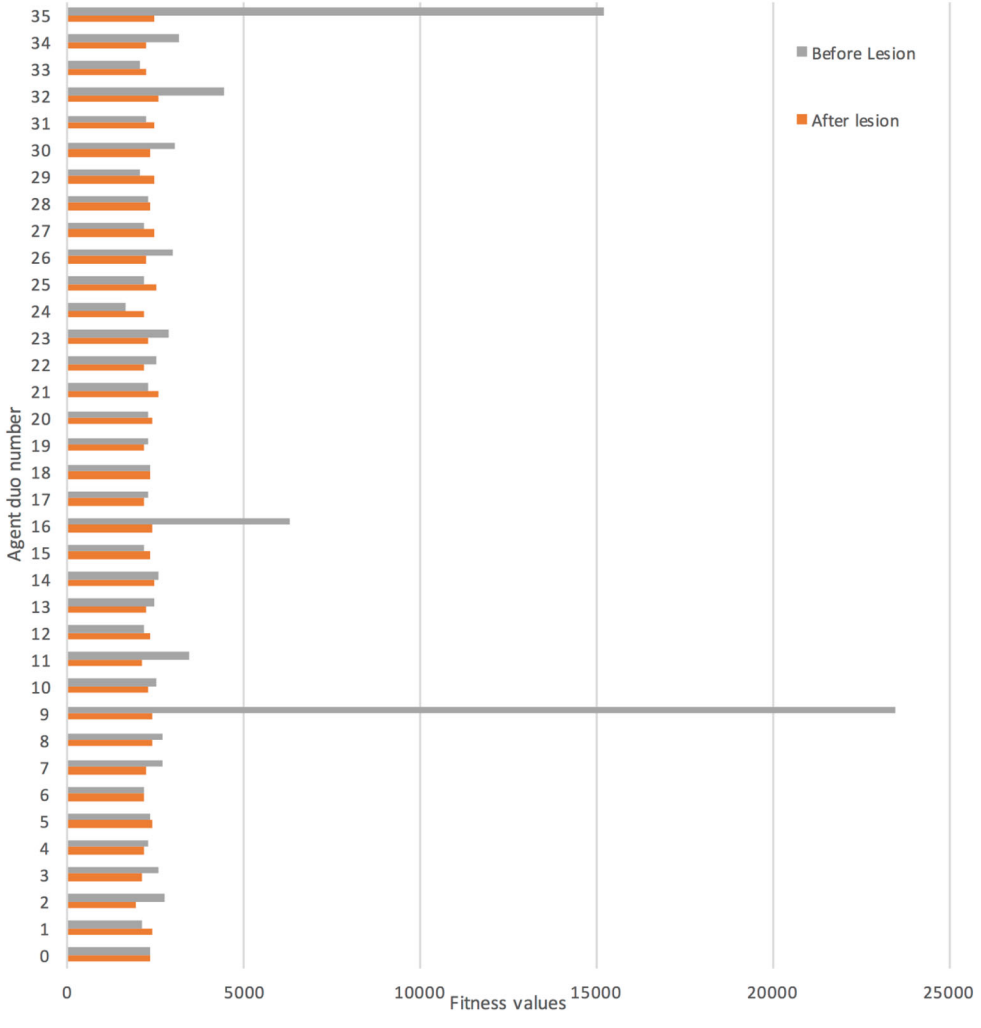

Figure 6. The fitness values per agent of the final population in Simulation 2 before (grey) and after (orange) lesioning the communicative connections.

Dual-agent behaviour in reduced environments

The mechanisms underlying the large benefit of communication were also analysed. We studied the behaviour of the fittest agents within three reduced environments (with food, predator, or no stimulus) in the presence or absence of a conspecific (see Figure 8). Agents exhibited (1) a general approach tendency towards conspecifics and (2) generalised avoidance of other stimuli, (3) often resonated with each other, producing intense, high-frequency oscillations, and (4) no straightforward differences in inter-agent communication appear to arise from stimuli with positive or negative valence. When approaching, agents would pass each other and then turned around to repeat this. This periodic behaviour could confuse predators and may explain part of the fitness advantage due to the communication ability. The tendency to avoid all stimuli meant that they would often end up starving to death (i.e. in the stimulus-free zone). To maintain fitness levels, it would suffice for the

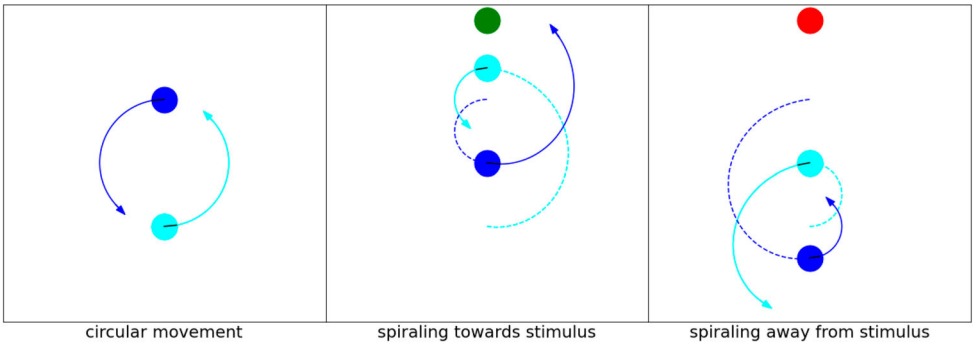

Figure 7. Three panels illustrating the periodic behaviours emerging in the pairs from Simulation 2. Left panel: Circular movement. Most agents (here blue and cyan, arrows indicating movement direction) circled each other (solid lines showing future movement, dashed lines showing past movement), persisting in such periodic movement until starvation. The circular movement helped to avoid predators as the agents formed an ever-moving target. Middle panel: In the presence of a food source, agents would tend to spiral towards the stimulus. Right panel: In the presence of a predator, pairs would spiral away from the stimulus.

agents to settle in predator-free zones and to move as little as possible in order not to waste energy. This also enhances the fitness-raising effect of approaching one's conspecific, because it would make the pair join in predator-free zones.

Inspecting the high-fitness agents in Figure 8, there are no apparent response differences between food and predator stimuli in the agent not being able to smell the stimulus directly, when either a food source or a predator is presented to the other agent (compare the second and sixth columns). This pair, therefore, does not appear to be able to differentially communicate stimulus valence over a longer distance. Stimulus presence or absence of a stimulus, regardless of valence (compare the fourth column with the second and sixth) is signalled to the conspecific, however. This virtual experiment thus reveals some kind of arousal communication (i.e. the presence of a relevant stimulus, irrespective of valence), but not affective communication.

Surprisingly, we did observe different responses of the pair as a whole (i.e. joint action; see Michael, 2011) to stimuli of different valence. Specifically, as can be seen in Table 1, the four highest-fitness agents spent more time in the food area and less time in the other areas than their lower-fitness peers, indicating a joint preference for food stimuli. The activations across all network layers across the two agents moreover, were synchronised throughout the simulations (but not completely identical). Affect contagion (cf, Michael, 2011) thus also seemed to occur, even to such an extent that there is continuous affect synchronisation, but this was not enacted by the communication scent.

Reduced neural network of the fittest pair

A pruned version of the network controlling the fittest agents was plotted to understand the neural dynamics and relate it to behaviour. Figure 9 shows the reduced network of pair 9, after having removed all connection strengths weaker in absolute value than 0.5 standard deviation below the absolute value of the mean. Treating excitatory and inhibitory connections as separate populations, gives thresholds of 0.92 (i.e. excitatory connections

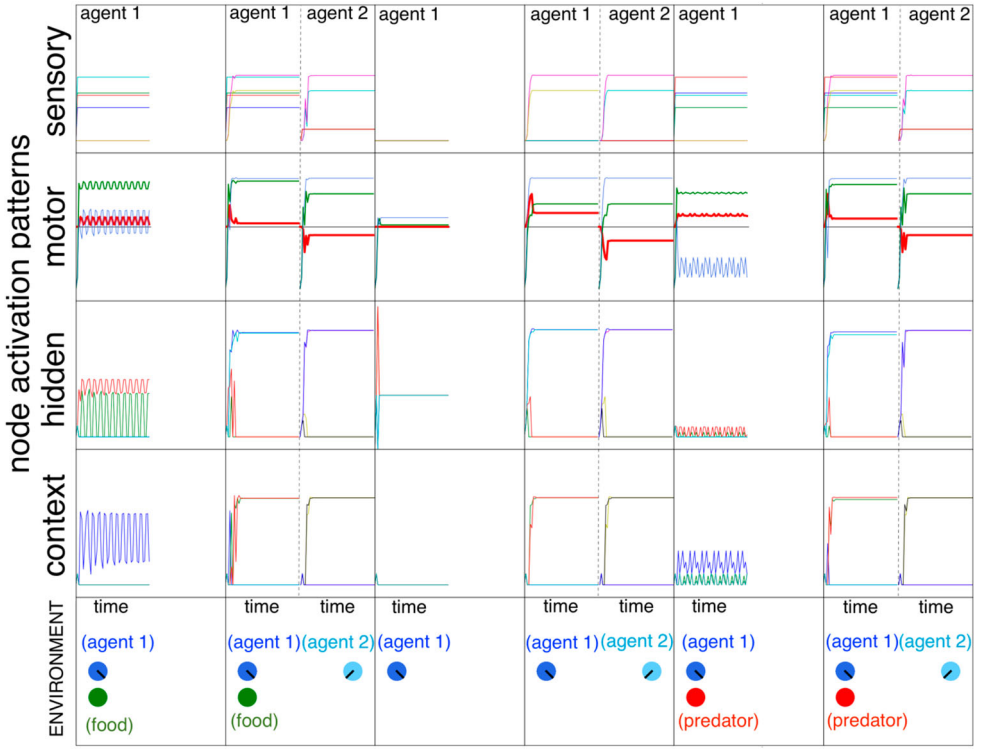

Figure 8. The responses from the agents of pair 9 (fitness value 23,463) to six different situations: food stimulus (columns 1 and 2), no stimulus (columns 3 and 4), predator stimulus (columns 5 and 6), both in the absence (columns 1, 3, and 5) and in the distant presence of a conspecific (columns 2, 4, and 6). The top four rows show the activations in input, output, hidden and context layers as a function of time, with the left and right part of each column showing, the activation of the first (dark blue) and the second agent (light blue), respectively. The bottom row shows a map of the testing environment.

below this strength are pruned) and −0.24 (i.e. inhibitory connections above this strength are pruned), respectively. Even in reduced form, the structure and dynamics of the network seem rather hard to disentangle.

We focus on three features of the network (i.e. competition, conflict monitoring, agent coupling) and provide a possible interpretation of its internal dynamics. In Figure 9a the left-most and right-most hidden-layer nodes (H_1 and H_4) competed with each other. H_1 had an excitatory connection to a context-layer node (C_3) that inhibited H_4 (conversely, H_4 had an excitatory connection to C_2 that inhibited H_1). This competition process by mutual inhibition also emerged in the simulations of Heerebout and Phaf (2010a, 2010b). They argued that this was a basic requirement for the modulation by neural oscillations to occur (see also Phaf & Rotteveel, 2012).

The approach response to the sender of the communication scent (see Figure 9b) was implemented both directly via input-output connections (E → O), and indirectly via the hidden layer (E → H → O). All connections in the indirect route between hidden layer nodes (H_{1-4}) and scent output (O_S) were excitatory. Thus, O_S activation would be maximal when the activity in H_{1-4} was maximal. H_1 and H_4 have a competitive relation to one

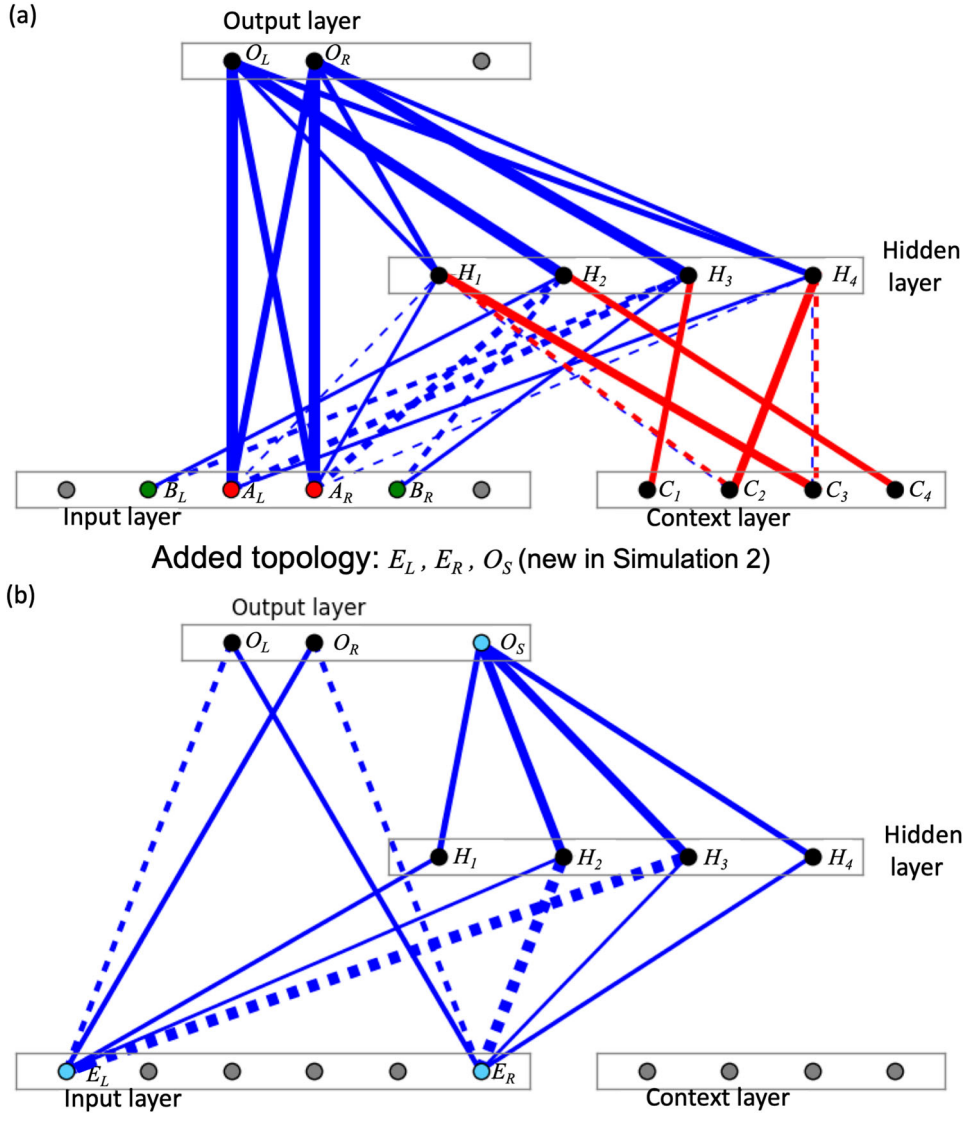

Figure 9. Reduced network of an agent from pair 9 with (a) showing only the non-communicative part as in Simulation 1, and (b) separately showing the communicative part added in Simulation 2. The plot shows forward-feeding (blue), and backward-feeding (red), excitatory (solid) and inhibitory (dashed) connections. The strength of the connections is indicated by width. Input nodes A, B, and E were mainly associated with predators (red), food (green), and conspecific (blue), respectively. Sub-scripts L and R indicate left and right.

another. During conflict, they inhibit each other, reducing the overall activity in H_{1-4}, and consequently that of OS. This node configuration, therefore, could function as a kind of conflict-monitoring module. H_1 and H_4 nodes are also heavily involved in stimulus processing so that the presence of a stimulus mitigates the approach to the conspecific. Stimulus-induced conflict (in H_{1-4}) reduces activation of O_S and consequently also lessens the approach response of the receiver agent due to the weaker communication scent input

from the sender. Given the high level of synchronisation between the agents' networks, conflict in H_{1-4} often occurs in both agents roughly simultaneously, reducing the tendency of both agents to approach each other. In other words, agents become less tightly coupled to each other when there is stimulus-induced conflict in their networks. The modulating mechanism of agent coupling may also help explain the stimulus-induced variations in the periodic behaviour patterns but the complexity of the connection scheme did not allow for any straightforward interpretation of these network dynamics.

General discussion

Two evolutionary simulations of simple organisms in a virtual environment filled with fitness-increasing, and decreasing, stimuli revealed the emergence of adaptive features related to affect coding (Simulation 1) and communication (Simulation 2). The simulations of Heerebout and Phaf (2010b) gave rise to the novel hypothesis that positive stimuli elicit higher frequency neural oscillations than negative stimuli. Neural oscillations also developed here, but a correspondence between positive/negative stimuli and high/low frequencies was only found in the highest fitness agent. Evolution gains it extremely powerful optimisation capacity from capitalising on the behaviour of a small number of fittest individuals, while neglecting the less fit individuals. The emergence of even a single very fit individual enables an escape from local fitness maxima and thus can trigger extensive further adaptations and exaptations.

Oscillatory mechanisms can emerge autonomously when the following requirements are met, (1) neural networks should allow for recurrent connections (with time delays in signal transmission, (2) there should be high levels of ambiguity between fitness-increasing and decreasing stimuli, and (3) fitness should be highly dependent on the ability to switch quickly between different responses. Heerebout and Phaf (2010a) indeed identified the modulation of attentional switching between competition winners as the primary function of neural oscillations, which implies that the affective coding by oscillations may itself have constituted an exaptation (Gould, 1991; Jacob, 1977; Shariff & Tracy, 2011). The above requirements may have been met frequently throughout evolutionary history, for many biological organisms. It is likely, therefore, that evolutionary tinkering has resulted in the more general emergence of affective coding by oscillations.

The setup was similar here to the one we aimed to replicate (Heerebout & Phaf, 2010ab), so these findings could still be related to details in the setup. For example, we only changed the genetic-algorithm procedure slightly by including the champion method. Further strengthening of these conclusions would require simulations with a strongly different setup while still meeting the above three requirements. Changes could be inspired by all properties and conditions that are expected to vary across organisms. Computing power allowing, possibilities are endless, and include, for instance, multiple modalities (e.g. sound and vision), different body shapes, different network architectures (but all involving recurrence), moving food sources, co-evolving predators, etc. It will also be interesting to have the network architecture itself evolve, to study whether, and which form of, recurrence emerges autonomously.

In Simulation 2, the setup was extended to one in which communication abilities between the agents could emerge. In the final generations, a fitness-increasing role for long-range communication indeed had developed. Based on observations in full and

reduced virtual environments, we noted that these agents showed a tendency to approach their conspecifics in a periodic fashion and to avoid all stimuli. In the fittest pairs, this coordinated pattern of movement was beneficial both in avoiding predators and conserving energy. The larger spiralling movements made by the agents in the presence of these stimuli, thwarted attempts of predators to catch one of them. Higher fitness pairs moreover, primarily tended to settle more in predator-free zones than lower fitness pairs.

Although oscillations resonating between the two networks were found in the final population, these did not appear to confer a fitness benefit. Our observations, therefore, do not lend support to an exaptation of neural oscillations for communication purposes. The adaptive function of oscillations identified by Heerebout and Phaf (2010ab) however, lies primarily in facilitating rapid switching between approach and avoidance actions. Because the different regions in the setup of Simulation 2 exclusively contained predators or food sources, or no stimuli at all, switching probably did not constitute a selection pressure here. Table 1, for instance, shows that all agents spent more than half of their time in the empty zones of the virtual environment. The low selection pressure for fast response switching could have led to optimizations away from oscillatory networks. In future simulation work, it would be interesting to configure environment setups still allowing for spatial coding, as in Simulation 2, while keeping evolutionary pressures on switching high. This could be done by allowing the foraging region to overlap with the predation zones.

In the virtual experiments performed on the final population, only a kind of arousal distinction (i.e. presence vs. absence) and no affective distinction (i.e. predator vs. food) was observed in the long-range communication between agents. This was probably due to the food and predators being separated in different zones. In the present setup, the most adaptive solution seems to be to join in predator-free zones. If a higher level of ambiguity were introduced in the environment by having predators in all zones, the coupling between agents could become less straightforward and the ability to communicate affective valence could have arisen. Because the agents mostly strived to remain within close vicinity, it seems plausible that the capacity for affective signalling from afar would not add much fitness. In the dynamic setting of the simulation, however, a different type of short-range affective communication emerged. When the agents were close by, they modulated each other's output and internal neural activity concerning the valence of nearby stimuli. This is typical of both affect detection and affect contagion (cf, Michael, 2011). The observed strength of internal and external coupling between agents suggests that short-range affect synchronisation would be a more fitting term.

The strong coupling between agents implied that, although possessing separate nervous systems, they were essentially behaving as if they had self-assembled into a single organism (cf, Couzin, 2009). They appeared to merge due to the communication scents acting as virtual connections between the networks. Collective behaviour as a consequence of communication abilities not only emerges in simulation studies (e.g. Ackland et al., 2007; de Greeff & Nolfi, 2010; Di Paolo, 2000), but is also very common in biological species, such as in foraging ants, swarms of insects, flocks of birds, and schools of fish. Each organism on itself has only relatively local sensing abilities that are extended by simple communication with conspecifics. In highly related grouping organisms, such as the social insects (e.g. ants, bees, wasps, etc.), collective cognition can be particularly sophisticated. Individual behaviour and interactions have evolved in these groups to benefit the colony's reproductive success, while strongly reducing inter-individual conflict. The functional integration

may have become so tight that they rightfully can be called "super-organisms" (Couzin, 2009). Arguably, this grouping behaviour in most species involves only minimal or no affect, but it seems to have been exapted emotionally into an adaptive action tendency "to tend and befriend" when threat is present, in humans at least (Taylor, 2006).

The analysis of the network dynamics in the fittest pair revealed that it involved competitive processing (as previously found by Heerebout & Phaf, 2010a). Moreover, the presence of competition in the hidden network layer directly reduced activation of the output scent that controlled the coordination between agents. The output scent, therefore, served as a conflict-monitoring signal, primarily transmitting the presence or absence of a stimulus, regardless of its valence, to the receiving agent. As competition seems to be one of the most basic information-processing mechanisms in the nervous system (e.g. Cerf et al., 2010; Duncan, 1996), it would be worthwhile to further explore the exaptation of conflict-monitoring for mutual communication and coordination between agents. In future work, one way to allow an affective distinction to become more clearly represented by conflict in the network could be to furnish the agents with more extensive processing capacities (i.e. more nodes and connections) and with lateral connections (i.e. allowing for direct mutual inhibition). The latter type of connections would make the jump to competitive processing more likely than in the present simulations, in which only indirect competition could develop. Future simulation work could also improve the exploratory setup of Simulation 2 by, for instance, increasing the evolutionary pressures for attentional competition and switching between winning responses.

The present study represents a, relatively novel, exercise in evolutionary cognitive neuroscience on small-scale quasi-neural networks in artificial environments, and aims to encourage the further bottom-up generation of theoretical hypotheses through evolutionary computation. Even with the current simplicity, the resulting network dynamics appeared to be complex. The insights into the organism's evolutionary development and internal processing gained from this type of computational simulation however, clearly expand the opportunities for analysis in affective neuroscience and emotion psychology. For interpretation, we made (1) observations of the agents' behaviour in their natural habitat, (2) in impoverished, static environments, (3) evolved a control population, (4) performed lesion studies, and (5) analysed abstracted networks. In biological organisms, such detailed analyses are often impossible.

These evolutionary simulations were designed to explore the emergence of affect and of communication in a bottom-up fashion. Previous evolutionary modelling suggested a novel hypothesis about core affect, which even renowned emotion theoreticians find hard to analyse (e.g. Frijda, 1986). Our mechanical analysis (Phaf & Rotteveel, 2012) is further strengthened here by the replication of crucial findings from these earlier simulations, at least with respect to the most adaptive solutions. A different type of communication developed than what was initially expected, but in hindsight makes good sense under these environmental pressures and agrees quite well with behaviour that can be observed in many biological species. All neural mechanisms employed by organisms and, accordingly, psychological processes, are contingent on their evolutionary history. Supplementing top-down cognitive theorising with bottom-up evolutionary computation, thus surely adds a useful instrument to the emotion theoretician's toolbox. Within given constraints, precise outcomes of evolutionary simulations are often unpredictable, very much like the results of biological evolution in nature. The fact that simulated evolution led us along a different

path for communication between agents than through neural oscillations illustrates the tinkering power of evolution.

Acknowledgement

CH is currently supported by the NWO Research Talent grant (no. 406.18.535).

Disclosure statement

The authors declare that the research was conducted in the absence of any commercial or financial relationships that could be construed as a potential conflict of interest.

Data Availability Statement

A Python (Jupyter notebook) version of the evolutionary model of affect we developed for this publication can be downloaded freely via Github (https://github.com/CasperHesp/evolution_neuralnets).

ORCID

Casper Hesp http://orcid.org/0000-0001-7669-4078
Bram T. Heerebout http://orcid.org/0000-0003-0767-270X
R. Hans Phaf http://orcid.org/0000-0002-7691-981X

References

Ackland, G. J., Hanes, R. D., & Cohen, M. H. (2007). Self-assembly of a model multicellular organism resembling the Dictyostelium slime molds. *arXiv preprint arXiv:0705*.0227.

Broekens, J., Jacobs, E., & Jonker, C. M. (2015). A reinforcement learning model of joy, distress, hope and fear. *Connection Science*, *27*(3), 215–233. https://doi.org/10.1080/09540091.2015.1031081

Burattini, E., & Rossi, S. (2010). Periodic activations of behaviours and emotional adaptation in behaviour-based robotics. *Connection Science*, *22*(3), 197–213. https://doi.org/10.1080/09540091003749691

Cerf, M., Thiruvengadam, N., Mormann, F., Kraskov, A., Quiroga, R. Q., Koch, C., & Fried, I. (2010). On-line, voluntary control of human temporal lobe neurons. *Nature*, *467*(7319), 1104–1108. https://doi.org/10.1038/nature09510

Cleveland, W. S. (1979). Robust locally weighted regression and smoothing scatterplots. *Journal of the American Statistical Association*, *74*(368), 829–836. https://doi.org/10.1080/01621459.1979.10481038

Couzin, I. D. (2009). Collective cognition in animal groups. *Trends in Cognitive Sciences*, *13*(1), 36–43. https://doi.org/10.1016/J.TICS.2008.10.002

Darwin, C. (1872). *The expression of emotions in man and animals*. Murray.

de Greeff, J., & Nolfi, S. (2010). Evolution of implicit and explicit communication in mobile robots. In *Evolution of communication and language in embodied agents* (pp. 179–214). Springer. https://doi.org/10.1007/978-3-642-01250-1_11

den Dulk, P., Heerebout, B. T., & Phaf, R. H. (2003). A computational study into the evolution of dual-route dynamics for affective processing. *Journal of Cognitive Neuroscience*, *15*(2), 194–208. https://doi.org/10.1162/089892903321208132

Di Paolo, E. A. (2000). Behavioral coordination, structural congruence and entrainment in a simulation of acoustically coupled agents. *Adaptive Behavior*, *8*(1), 27–48. https://doi.org/10.1177/105971230000800103

Drake, J. W., Charlesworth, B., Charlesworth, D., & Crow, J. F. (1998). Rates of spontaneous mutation. *Genetics*, *148*, 1667–1686.

Duncan, J. (1996). Cooperating brain systems in selective perception and action. In T. Inui, & J. L. McClelland (Eds.), *Attention and Performance XVI* (pp. 549–578). MIT Press.
Fridlund, A. J. (1994). *Human facial expression: An evolutionary view*. Academic Press.
Frijda, N. H. (1986). *The emotions*. Cambridge University Press.
Goldberg, D. E. (1989). *Genetic algorithms in search, optimization and machine learning*. Addison-Wesley.
Gould, S. J. (1991). Exaptation: A crucial tool for evolutionary psychology. *Journal of Social Issues*, *47*(3), 43–65. https://doi.org/10.1111/j.1540-4560.1991.tb01822.x.
Heerebout, B. T., & Phaf, R. H. (2010a). Emergent oscillations in evolutionary simulations: Oscillating networks increase switching efficacy. *Journal of Cognitive Neuroscience*, *22*(5), 807–823. https://doi.org/10.1162/jocn.2009.21205
Heerebout, B. T., & Phaf, R. H. (2010b). Good vibrations switch attention: An affective function for network oscillations in evolutionary simulations. *Cognitive, Affective, & Behavioral Neuroscience*, *10*(2), 217–229. https://doi.org/10.3758/CABN.10.2. 217
Heerebout, B. T., Tap, A. Y., Rotteveel, M., & Phaf, R. H. (2013). Gamma flicker elicits positive affect without awareness. *Consciousness and Cognition*, *22*(1), 281–289. https://doi.org/10.1016/j.concog.2012.07.001
Jacob, F. (1977). Evolution and tinkering. *Science*, *196*(4295), 1161–1166. https://doi.org/10.1126/science.860134
Johnston, V. (2003). The origin and function of pleasure. *Cognition and Emotion*, *17*(2), 167–179. https://doi.org/10.1080/02699930302290
Kounios, J., & Beeman, M. (2009). The Aha! moment: The cognitive neuroscience of insight. *Current Directions in Psychological Science*, *18*(4), 210–216. https://doi.org/10.1111/j.1467- 8721.2009.01638.x
LeDoux, J. E. (1996). *The emotional brain*. Simon & Schuster.
Lowe, R., Humphries, M., & Ziemke, T. (2009). The dual-route hypothesis: Evaluating a neurocomputational model of fear conditioning in rats. *Connection Science*, *21*(1), 15–37. https://doi.org/10.1080/09540090802414085
Magnani, L., & Bertolotti, T. (Eds.). (2017). *Springer handbook of model-based science*. Springer. https://doi.org/10.1007/ 978- 3- 319- 30526- 4
Marco-Pallarés, J., Münte, T. F., & Rodríguez-Fornells, A. (2015). The role of high-frequency oscillatory activity in reward processing and learning. *Neuroscience & Biobehavioral Reviews*, *49*, 1–7. https://doi.org/10.1016/j.neubiorev.2014.11.014
Michael, J. (2011). Shared emotions and joint action. *Review of Philosophy and Psychology*, *2*(2), 355–373. https://doi.org/10.1007/s13164-011-0055-2
Minelli, A., Chagas-Júnior, A., & Edgecombe, G. D. (2009). Saltational evolution of trunk segment number in centipedes. *Evolution & Development*, *11*(3), 318–322. https://doi.org/10.1111/j.1525-142X.2009.00334.x. URL
Phaf, R. H., Mohr, S. E., Rotteveel, M., & Wicherts, J. M. (2014). Approach, avoidance, and affect: A meta-analysis of approach-avoidance tendencies in manual reaction time tasks. *Frontiers in Psychology*, *5*, 378. https://doi.org/10.3389/fpsyg.2014.00378
Phaf, R. H., & Rotteveel, M. (2012). Affective monitoring: A generic mechanism for affect elicitation. *Frontiers in Psychology*, *3*, 47. https://doi.org/10.3389/fpsyg.2012.00047
Reggia, J. A., Schulz, R., Wilkinson, G. S., & Uriagereka, J. (2001). Conditions enabling the evolution of inter-agent signaling in an artificial world. *Artificial Life*, *7*(1), 3–32. https://doi.org/10.1162/106454601300328007
Shariff, A. F., & Tracy, J. L. (2011). What are emotion expressions for? *Current Directions in Psychological Science*, *20*(6), 395–399. https://doi.org/10.1177/0963721411424739. URL
Strongman, K. T. (1996). *The psychology of emotion: Theories of emotion in perspective* (4th ed.). John Wiley & Sons.
Taylor, S. E. (2006). Tend and befriend. *Current Directions in Psychological Science*, *15*(6), 273–277. https://doi.org/10.1111/j.1467- 8721

Tsai, H. C., Zhang, F., Adamantidis, A., Stuber, G. D., Bonci, A., De Lecea, L., & Deisseroth, K. (2009). Phasic firing in dopaminergic neurons is sufficient for behavioral conditioning. *Science*, *324*(5930), 1080–1084. https://doi.org/10.1126/science.1168878

van Rossum, G., & Drake, F. L. (2001). *Python reference Manual*. Amsterdam: Centrum voor Wiskunde en Informatica. https://docs.python.org/2.0/ref/ref.html.

Wöhr, M., van Gaalen, M. M., & Schwarting, R. K. (2015). Affective communication in rodents: Serotonin and its modulating role in ultrasonic vocalizations. *Behavioural Pharmacology*, *26*(6), 506–521. https://doi.org/10.1097/FBP.0000000000000172

Appendices

Appendix A. Scent intensity

In Simulation 1, the scent intensity as a function of distance to the source 1 is given by:

$$S(d) = S_{max}\frac{1 - d/d_{max}}{1 + d} if d < d_{max}$$

Where the maximum intensity is $S_{max} = 25$ and the maximum distance is $d_{max} = 100$, in code units. S(d) is zero for d larger than d_{max}. We plot this function for the relevant range between touch ($d = 20$) and $d_{max} = 100$:

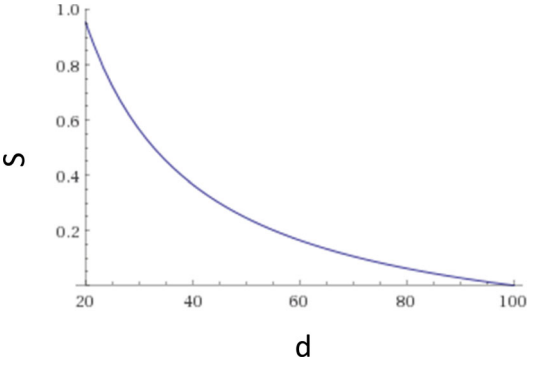

Appendix B. Random mutation size

The random mutation size X in Simulation 1 is calculated using the following distribution:

$$X = m\log(1/r - 1)$$

Where the average mutation size $m = 0.1$ and r is a random number between 0 and 1. Note that mutations can be positive or negative. We plot the mutation size as a function of *r*:

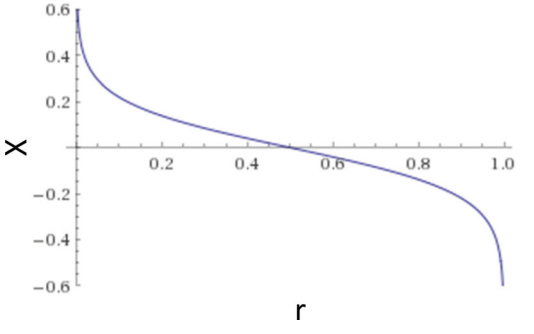

Appendix C. Probability of passing into the next generation

For every agent, the probability of passing into the next generation is calculated in two steps. It is first calculated as follows for an agent i, based on its fitness:

$$p_{1,i} = (1 - p_{min})\frac{f_i - f_{min}}{f_{max} - f_{min}} + p_{min}$$

where the minimum probability $p_{min} = 0.15$, f_i is the fitness of agent I, and f_{max} and f_{min} are the maximum and minimum fitness in the population. As an illustration, we plot the probability of survival as a function of f_i for a population with $f_{min} = 1000$ and $f_{max} = 3000$.

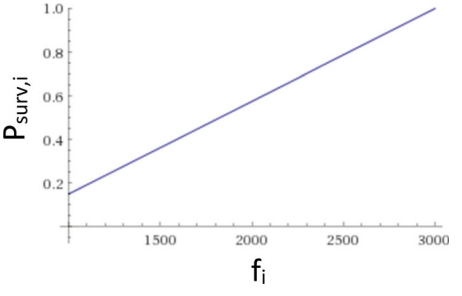

Subsequently, this probability is modulated to control changes in the population size (keeping it around the initial size). If the current population size, n_{cur}, is larger than the initial population size, $n_{init} = 18$ agents, the probability of continuing into the next generation becomes:

$$p_{2,i} = \frac{n_{init}}{n_{cur}} p_{1,i}$$

When n_{cur} is larger than or equal to n_{init}, the probability becomes:

$$p_{2,i} = 1 - (1 - p_{1,i})\left(1 - \left(1 - \frac{n_{cur}}{n_{init}}\right)^2\right)$$

Below, we plot both probability distributions as a function of n_{cur} for the case that $p_{1,i} = 0.3$. Note that both distributions converge to $p_{2,i} = 0.3$ when $n_{cur} = n_{init} = 18$.

Appendix D. Communication scent intensity

In Simulation 2, the communication scent intensity as a function of distance between the agents is:

$$S_{com}(d) = 1.91 + 0.0180d - 0.0009d^2$$

This equation holds for distances until 50 code units. Beyond that distance, the smell intensity is the same as at $d = 50$. Note that the directional sensitivity (slope of the function) increases with larger distances. We plot the scent intensity S_{com} as a function of distance.

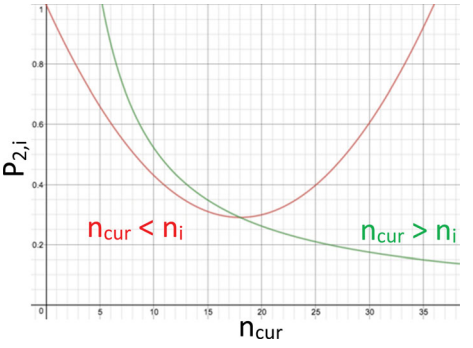

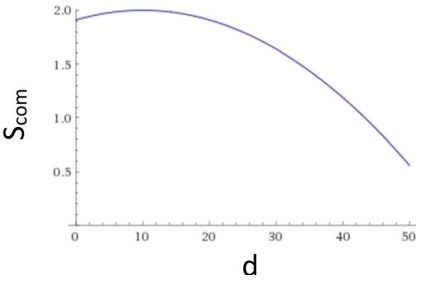

Appendix E. List of parameters in the setups of simulations 1 and 2

		Simulation 1	Simulation 2
Environment	Size	(40 × 40)	(60 × 60)
	Initial population size	18	18 pairs
	Number of food sources	10	4
	Number of predators	6	4
	Number of agents	1	2
	Object radius	1	1
	Scent intensity S as a function of distance d	$S(d) = 25\frac{1-d/10}{1+d} if d < 10$	
	Communication signal intensity S_{com} as a function of distance d		$S_{com}(d) = 1.91 + 0.0180d - 0.0009d^2$
	Input activation function	$I = \frac{\sum S_i}{1+\sum S_i}$.	
	Angle between nostrils	90 degrees	
	Angle between motor actuators	180 degrees	
Agent settings	Initial energy level	5	5
	Energy loss per time step	∼0.001	∼0.001
	Initial location	random	random in top left area (20 × 40) random in bottom right area (40 × 20)
	Number of sensory nodes	2 (scent A) 2 (scent B)	2 (scent A) 2 (scent B) 2 (scent E)
	Number of motor nodes	2 (left/right $O_{L/R}$)	

(*continued*)

		Simulation 1	Simulation 2
	Acceleration	$\vec{a} = 2\min(O_L, O_R)\begin{pmatrix}\cos\theta\\ \sin\theta\end{pmatrix}$	
	Velocity	$\vec{v}_{t+1} = 0.98\vec{v}_t + \vec{a}\Delta t$	
	Location	$\vec{x}_{t+1} = \vec{x}_t + \frac{1}{2}(\vec{v}_{t+1} + \vec{v}_t)\Delta t$	
	Angular acceleration	$\alpha = 0.4(O_L - O_R)$	
	Angular velocity	$\omega_{t+1} = 0.98\omega_t + \alpha$	
	Angular orientation	$\theta_{t+1} = \theta_t + \frac{1}{2}(\omega_{t+1} + \omega_t)$	
	Number of scent output nodes	0	1
	Number of hidden nodes	4	4
	Number of context nodes	4	4
	Number of unique connections (due to symmetry)	64	80
	Initial connection weights $\vec{w}_i$	all connections zero	fittest agent of simulation 1
	Emission intensity scent C		1
	Emission intensity scent E	0	1
Plant settings	Energy content		1
	Initial location	random	random in bottom left area (20×20)
	Intensity scent A	1.0	1.0
	Intensity scent B	0.5	0.5
Predator settings	Initial location	random	random in top right area (40×40)
	Emission intensity scent A	0.5	0.5
	Emission intensity scent B	1	1
	Emission intensity scent D	1	1
	Number of input nodes (left/right: $I_{L/R}$)	2 (scent C: $I_{C,L/R}$)	2 (scent C)
	2 (scent D: $I_{D,L/R}$)	2 (scent C)	
	Number of motor nodes	2 ($O_{L/R}$)	2
	Number of unique connections (due to symmetry)	4	4
	Connections $I_{C,L/R} \rightarrow O_{R/L}$	3	
	Connections $I_{C,R/L} \rightarrow O_{R/L}$	-0.1	
	Connections $I_{D,L/R} \rightarrow O_{R/L}$	-0.02	
	Connections $I_{D,R/L} \rightarrow O_{R/L}$	0.6	
Genetic algorithm	Initial population size	18	18 pairs
	Number of genes	64	72
	Number of generations	$\sim$ 10,000	$\sim$ 10,000
	Fitness function	$f = E \cdot T_{life}$	$f = E_1 \cdot E_2 \cdot T_{life}$
	Base probability of survival	$p_{surv,0} = 0.15 + 0.85\frac{f - f_{min}}{f_{max} - f_{min}}$	
	Probability of survival if $n \leq n_{init}$	$p_{surv} = \frac{n_{init}}{n}p_{surv,0}$	
	Probability of survival if $n > n_{init}$	$p_{surv} = 1 - (1 - p_{rep,0})\left(1 - \left(1 - \frac{n}{n_{init}}\right)^2\right)$	
	Number of trials per agent	12	
	Parent 1: Tournament selection	Fittest of random subset (1/3rd of total population)	
	Parent 2: Selection probability	$p_{parent} \propto f/\Delta_{12}$	
	Distance between connection weights of parents 1 and 2 ($\vec{w}_1, \vec{w}_2$)	$\Delta_{12} = \sum \lvert\vec{w}_2 - \vec{w}_1\rvert$	
	Crossover probability	0.5	
	Number of crossover genes	2 (randomly selected)	
	Mutation size X	$X = m\log(1/r - 1)$, where r is drawn from [0,1]	
	Average mutation size m	0.1	0.01 for genes not involved in communication 0.2 for communication genes